

# Proton and Electron Transfer Mechanisms in the Formation of Neutral and Charged Quinhydrone-Like Complexes: A Multilayered Computational Study

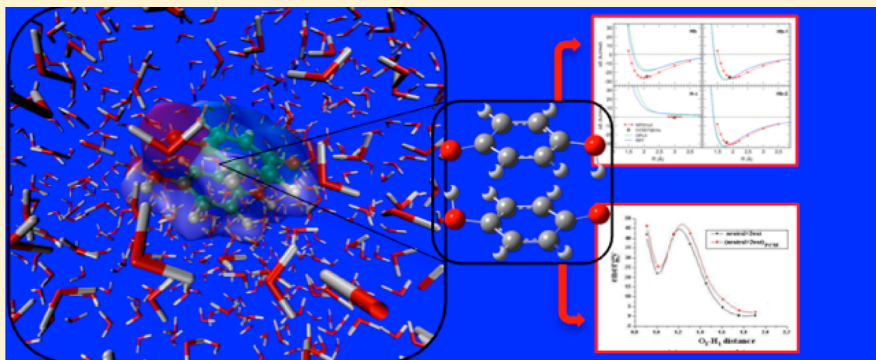
Vincenzo Barone,<sup>†</sup> Ivo Cacelli,<sup>‡</sup> Alessandro Ferretti,<sup>§</sup> Giacomo Prampolini,<sup>§</sup> and Giovanni Villani<sup>\*,§</sup>

<sup>†</sup>Scuola Normale Superiore, Piazza dei Cavalieri 7, I-56126 Pisa, Italy

<sup>‡</sup>Dipartimento di Chimica e Chimica Industriale, Università di Pisa, Via Risorgimento 35, I-56126 Pisa, Italy

<sup>§</sup>Istituto di Chimica dei Composti OrganoMetallici (ICCOM-CNR), Area della Ricerca, via G. Moruzzi 1, I-56124 Pisa, Italy

## Supporting Information



**ABSTRACT:** The redox and proton transfer processes involving the several dimers arising from quinones are studied by quantum mechanical methods using second order perturbation theory (MP2) and a medium size basis set optimized for reproducing dispersion interactions. Furthermore, bulk solvent effects are taken into account by the polarizable continuum solvent (PCM) approach possibly integrated by two explicit water molecules for an improved description of the cybotactic region. Our results indicate that several neutral and anionic dimers are kept together mainly by strong hydrogen bonds, but dispersion forces introduce additional non-negligible effects. The computed energy paths indicate that a proton transfer process should accompany the two-electron reduction of quinhydrone and that two dimers in the reduced form can be simultaneously present in solution, in agreement with available experimental data.

## INTRODUCTION

Due to their ubiquity in biologically relevant processes, quinone species and their derivatives have attracted a great attention, both from a theoretical and an experimental point of view.<sup>1–15</sup> Over the last decades, major interest was focused on the basic action of quinones in controlling normal electron transfer (ET) through electron carriers, proton transfer (PT), and charge separation across membranes.<sup>16</sup> PT and ET concerted mechanisms (e.g., proton-coupled electron transfer, PCET<sup>17</sup>) play a relevant role in many systems of biological interest, like mitochondria, chloroplasts, or cell membranes. In spite of the large number of studies devoted to the general aspects of concerted transfers,<sup>18,19</sup> there is still debate about a precise definition of the process involving both proton and electron transfer.<sup>20–23</sup> There is also a type of pathway in which concerted electron–proton transfer occurs, involving more than one site. In this case, the term multiple site-electron proton transfer (MS-EPT) has been introduced<sup>24</sup> to indicate an electron–proton donor simultaneously transferring electrons and protons to different acceptors, or an electron–proton

acceptor simultaneously accepting electrons and protons from different donors. This MS-EPT process appears to be the biological pathway in which long-range electron transfer<sup>25</sup> is coupled to short-range proton transfer. The coupling between the transfer of electron and proton has been found to be effective in the G-C Watson–Crick base pair, where the addition of electron or hydride is capable to trigger the proton transfer.<sup>26–28</sup> In the A-T and G-C base pairs, both in vacuum<sup>29,30</sup> and hydrated,<sup>31,32</sup> the formation of imino-enol tautomers is a possible mechanism of hydrogen atoms transfer.

Among the three main families of naturally occurring quinones (benzoquinones, naphthoquinones, and anthraquinones<sup>33</sup>), we will focus our attention on benzoquinones (Scheme 1), whose ET sequence is driven by the redox potential of a quinone (Q) interconverting into hydroquinone (H<sub>2</sub>Q). A number of studies were devoted in the past to the characterization of the effects of protonation on the redox

Received: August 27, 2014

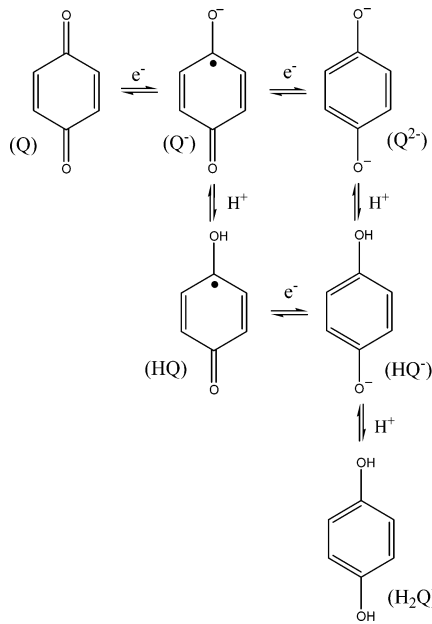
Published: October 9, 2014



ACS Publications

© 2014 American Chemical Society

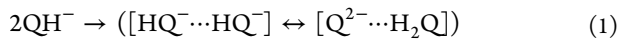
**Scheme 1. Monomers Considered in the Formation of Quinhydrone-Like Dimer Complexes and Their Redox and Protonation Equilibria: *p*-Benziquinone (Q); Hydroquinone ( $H_2Q$ ); Semiquinone ( $HQ^-$ ); Hydroquinone Anion ( $HQ^{2-}$ ); Hydroquinone Di-Anion ( $Q^{2-}$ )**



potential of various quinones, both in protic and aprotic solvents.<sup>2–4,9,11</sup> The detection of both neutral ( $H_2Q$ ) and anionic ( $HQ^-$  and  $Q^{2-}$ ) structures and their complexes is one of the main results of these studies.

In aprotic solvents, the electrochemical reduction occurs following two reversible or quasi-reversible consecutive electron transfer steps.<sup>6,7</sup> Under these conditions, the dianion  $Q^{2-}$  is stable and can be directly detected on the reverse scan in cyclic voltammetry experiments. Interestingly, when excess concentrations of proton donors are employed in aprotic solvents,<sup>1–3,11,34</sup> a strong interacting complex between the reduced species ( $H_2Q$ ) and the donor anion was found.

For the formation of such kind of complexes, a two electron–two proton transfer mechanism has been proposed for the redox process in a wide variety of quinones.<sup>10,11,13,35</sup> However, when the concentrations of the quinone species and the donor are similar, a different mechanism has been recently proposed.<sup>35</sup> In fact, the appearance<sup>36</sup> in voltammetric waves of a broad peak, positioned between those expected for  $Q^{2-}$  and  $Q^\bullet$ , could not be explained in the two electron–two proton transfer scheme, rather it was rationalized in ref 35 by hypothesizing the formation of an anionic dimer complex  $[Q^{2-}\cdots H_2Q]$ , similar in structure to the well-known quinhydrone  $[Q\cdots H_2Q]$ . Both cyclic voltammetry and  $^1H$  NMR experiments reported in that article confirmed the formation of such a complex, indicating that the  $QH^-$  species undergoes the reaction:



Unfortunately, experimental techniques<sup>35</sup> were not able to characterize the dimeric structure, nor to discriminate the position of the hydrogen atoms within the complex. The authors, underlining the possible mixed nature of reaction 1 as intermediate between proton transfer and disproportionation (see also Scheme 1), hypothesized that an approximately face-

to-face (FF) anionic dimer could be stabilized by strong hydrogen bond (HB) interactions, and attempted to characterize the involved  $[QH^- \cdots QH^-]$  and  $[Q^{2-} \cdots H_2Q]$  dimer complexes and their interconversion path (1) through quantum mechanical (QM) calculations. These calculations, based on the density functional theory (DFT) with different functionals, indicated the  $[QH^- \cdots QH^-]$  complex to be more stable than  $[Q^{2-} \cdots H_2Q]$  by  $\sim 80$  kJ mol<sup>-1</sup>, with an interconversion activation energy of 108.4 kJ mol<sup>-1</sup>.<sup>35</sup> Despite the authors' conclusion that the interconversion between the two complexes is possible, as it could be driven by thermal effects, it seems that the computed activation energy is too large to allow for a thermal activation process at 298 K.

Very recently, a computational revisit of the structural and spectroscopic features of quinhydrone was performed by our group,<sup>37</sup> with the aim of validating an accurate yet computationally effective approach for the characterization of such kind of complexes. It turned out that the implementation of a modified basis set within the Möller–Plesset second order perturbation theory (MP2), is capable to account well for all contributions to the interaction energy, providing an accuracy comparable to that of the very reliable (but computationally too demanding) Coupled-Cluster CCSD(T) model extrapolated to the complete basis set (cbs) limit.<sup>38</sup> Conversely, the MPW1B95 DFT functional, proposed for quinhydrone in ref 39 and successively employed in ref 35, was found to severely underestimate the dispersion interaction occurring between the stacked rings. Indeed, both CCSD(T) and MP2 results indicated that both HB and dispersion forces play a crucial role in the stabilization of quinhydrone-like dimer complexes.<sup>37</sup> Because the  $\pi$ – $\pi$  interactions, responsible for the dispersion energy, are found to be dependent not only from the inter ring separation but also from the relative orientation of the two moieties, it can be speculated that a correct assessment of such interaction could change the description of the interconversion path (1) reported in ref 35, eventually leading to better agreement with the experimental findings. Although semi-empirical dispersion models are available to complement semilocal density functionals,<sup>40</sup> we preferred to employ the wave-function-based MP2 approach with modified basis sets (previously validated in the study of quinhydrone complexes in vacuo) to perform a computational investigation on dimer complexes possibly involved in the PT and ET mechanisms. Moreover, to gain a deeper insight on the role of solvation, calculations were performed in different solvents, namely, water, acetonitrile (ACE), and dimethyl sulfoxide (DMSO).

The main goal of this paper is to achieve a reliable description of the considered complexes and of the transfer mechanisms occurring within the dimers. In particular, three issues should be addressed: (i) what is transferred along the H-bridge (i.e., a hydrogen atom or a proton), (ii) which is the mechanism of this transfer, (iii) how the solvent influences this mechanism. Finally, the conclusions drawn from the computational analysis, will be discussed in the light of experimental evidence reported in ref 35.

## ■ COMPUTATIONAL DETAILS

**QM Calculations.** Calculations are performed at the CCSD(T) and MP2 level of theory with the Gaussian09 package.<sup>41</sup> In the first case, the cbs energy is estimated following the procedure described in detail in ref<sup>42</sup> and denoted here as CCSD(T)@cbs. In the MP2 calculations, all neutral and charged quinone species are described through the

same 6-31G\* modified basis set, previously validated for quinhydrone in vacuo<sup>42</sup> where, in order to accurately account for the dispersion energy, the polarization exponents for carbon and oxygen atoms are optimized to 0.25 and 0.44, respectively; this computational model will be referred to as MP2mod in the following. When the solvent (H<sub>2</sub>O, ACE or DMSO) is included, the standard polarizable continuum solvent (PCM)<sup>43</sup> approach is adopted. Additionally, because H<sub>2</sub>O is a protic solvent which may form strong HBs with the quinoid species, we decided to consider the local nature of the interaction. For this reason, few explicit molecules are also considered (*vide infra*) in MP2 calculations. Water molecules are described by the standard 6-31G\* basis set, where the oxygen polarization exponent has the standard value of 0.80. This choice was made in view of the fact that the reduction of the basis set polarization exponents in MP2 is advisable when dispersion forces have a major role in the binding energy.<sup>44–53</sup> Conversely, when the interaction is governed by electrostatic zero- or first-order contributions (e.g., polarization) no correction of the basis set is needed.

In order to study PT within the investigated complexes, calculations are performed by fixing one O–H distance at several different values and optimizing all the remaining internal coordinates. This allows to build the minimum energy path (MEP) of the multidimensional potential energy surface (PES) from OH···O to O···HO, that is, the PT from a monomer to the other one. As no other constraint is imposed to the dimer geometry, all possible movements of the OHO group are allowed, including the change of the OHO angle. Conversely, if the relaxation of the other coordinates is neglected, a large hysteresis and an overestimated energy barrier can result, as shown for instance in refs 35,54.

**MD Simulations.** To reliably select the number of solvating water molecules to be explicitly considered in QM calculations, molecular dynamics (MD) simulations were performed on a quinhydrone complex surrounded by 1194 water molecules described with the well-known Tip3p force field.<sup>55,56</sup> The intramolecular parameters of *p*-benzoquinone and hydroquinone were obtained through the JOYCE<sup>57,58</sup> procedure, fitting QM reference data (i.e., energies, gradient and Hessian matrix) purposely computed at the B3LYP/cc-pvDz level. Intermolecular interactions involving *p*-benzoquinone and hydroquinone were taken from the OPLS force field,<sup>59</sup> except for some Lennard-Jones (LJ) parameters which were further refined to better match the QM computed interaction energy curves (see next section). Throughout the text, final parameters will be referred as Refined Force Field (RFF).

All simulations were performed with the GROMACS software.<sup>60</sup> The starting configuration was obtained by solvating a stacked dimer, whose geometry was previously optimized at MP2mod level;<sup>37</sup> next the geometry of the whole system was fully optimized through the steepest descent method implemented in the GROMACS engine.<sup>60</sup> Because we are interested in sampling the solvation sphere around the quinhydrone complex (and not that of the separated monomers), the center of mass of quinhydrone complex resulting after the minimization was constrained, to avoid configurations where the two monomers are too far apart. Starting with such a configuration, the simulations were carried out for 10 ns in the NPT ensemble at 1 atm and 298 K. Both temperature and pressure were kept constant through the Berendsen weak coupling scheme. In all simulations, a time step of 0.2 fs was employed, to correctly account for fast CH

and OH vibrations. The solvation shells around the complex were analyzed in terms of the pair correlation function (pcf)  $g(r)$  between the center of mass of quinhydrone and that of the surrounding water molecules. Several configurations were randomly selected from the final MD trajectory, and for each of them, the quinhydrone complex was extracted together with the closest water molecules. As detailed in the following, these sorted arrangements were then used as a starting point for energy minimizations with a different number of water molecules, in order to assess how many water molecules are needed for a reliable investigation of the solvated quinhydrone complex.

## RESULTS AND DISCUSSION

**Basis Set Validation.** In previous work,<sup>37</sup> we were able to obtain a close matching between MP2mod and CCSD(T)@cbs

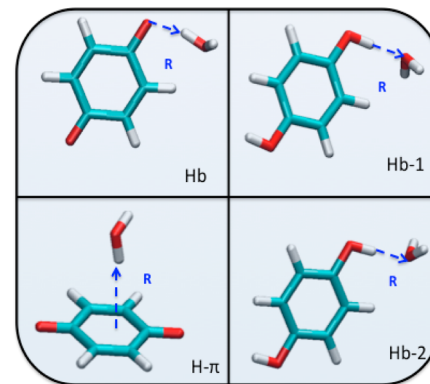


**Figure 1.** *p*-Benzoquinone/water (Q + H<sub>2</sub>O, left) and hydroquinone/water (H<sub>2</sub>Q + H<sub>2</sub>O, right) complexes considered for the basis set validation of the MP2mod calculation. Labels refer to the prevalent interaction type between the two species, either HB (namely, Hb, Hb-1, Hb-2 complexes) or H-π.

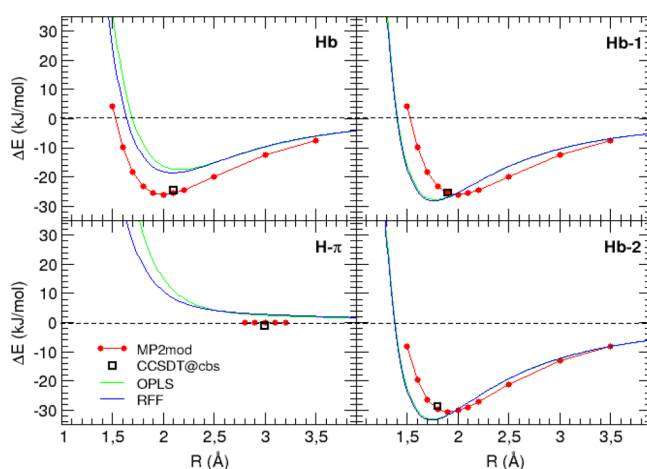


**Figure 2.** *p*-Benzoquinone/water (Q + H<sub>2</sub>O, left) and hydroquinone/water (H<sub>2</sub>Q + H<sub>2</sub>O, right) complexes considered for the basis set validation.

binding energies of hydroquinone dimers in different arrangements by optimizing the exponents of the polarization functions of non-hydrogen atoms starting from their 6-31G\* values. However, this test was performed only on quinhydrone in vacuo, whereas no information is available on the accuracy of the MP2mod approach to represent interactions of quinones

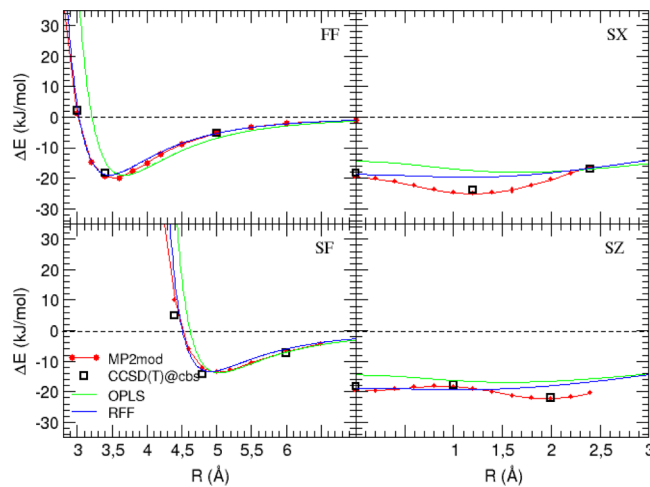


**Figure 3.** Quinhydrone interaction curves for selected arrangements. Labels (see Figure S1 in Supporting Information) refer to ref 37, where the QM curves (MP2mod and CCSD(T)@cbs, red circles and black squares, respectively) are also reported. OPLS and RFF energies are computed in this work and displayed with green and blue lines.

with water molecules. Therefore, a further validation of the MP2mod approach was performed for selected configurations of *p*-benzoquinone–water and hydroquinone–water complexes. Among all investigated geometries, two arrangements for each species were chosen, where the water molecule is interacting with the organic species either by HB or by H–π interactions. The considered structures, corresponding to the most probable arrangements according to preliminary simulations, are displayed and labeled in Figure 1.

MP2mod interaction energy curves were then obtained for each arrangement, by varying stepwise the coordinate R (shown in Figure 1), defined as the distance between the O and H atoms involved in the HB or, in the case of the H–π interactions, as the distance between the nearest water H atom and the center of the quinone ring. The resulting MP2mod curves, shown in Figure 2, display a very reasonable scenario. Indeed, it appears that the main source of attraction between water and both quinoid species is the HB force, whereas the interaction of the H–π type is always repulsive. To quantitatively validate the MP2mod results, four geometries, one for each arrangement, were selected and the corresponding interaction energies were computed at CCSD(T)@cbs level. By looking at Figure 2, where the CCSD(T)@cbs values are also reported, it appears that the MP2mod energies are in excellent agreement with their higher level counterparts. Therefore, the

computationally cheap method MP2mod can be confidently adopted to handle also the interaction of the quinoid species with water. The OPLS and RFF curves in Figure 1 will be discussed in a subsequent section.

Finally, it can be also assumed that in the case of charged structures, as for instance the dianionic complexes [QH<sup>−</sup>⋯QH<sup>−</sup>] and [Q<sup>2−</sup>⋯H<sub>2</sub>Q], the type of forces involved should be of the same nature as those in the neutral form [Q⋯H<sub>2</sub>Q], that is, π–π stacking interaction and HB. This was also verified with some test calculations on [QH<sup>−</sup>⋯QH<sup>−</sup>] (see Figure S4 in the SI), which showed the same level of accuracy as that on the corresponding neutral dimer. Therefore, the polarization exponents determined in the previous paper<sup>37</sup> for the neutral complexes can be extended to the charged ones.

**FF Validation.** One of the goals of the present work is to investigate the role of solvent (protic and aprotic) on the stability not only of the neutral quinhydrone complex but also of its charged redox derivatives, like [QH<sup>−</sup>⋯QH<sup>−</sup>] and [Q<sup>2−</sup>⋯H<sub>2</sub>Q] equilibria. In a first approximation, aprotic solvents (here ACE and DMSO) can be modeled by a polarizable continuum (PCM), but the most care is needed concerning specific short-range interactions between the solute and water. In fact, strong specific interactions as HB can be established between the solute and neighboring water molecules, whose role should be taken into account explicitly when evaluating the stability of the dimer complex, also considering the possibility that water protons are directly involved in the PT/ET mechanisms.

The first problem is then to define a minimum number of solvent molecules, to reliably account for the embedding medium at a reasonable computational cost. The most natural way to investigate the local solvation environment is resorting to classical MD simulation. However, the picture available through MD sampling is dependent on the adopted FF. The FF parameters (both LJ and point charges) for the organic moieties were initially taken from the OPLS FF,<sup>59,61</sup> although the Tip3P model<sup>55,56</sup> was adopted for the water molecules. The accuracy of this intermolecular description, describing the Q/H<sub>2</sub>Q, Q/H<sub>2</sub>O and H<sub>2</sub>Q/H<sub>2</sub>O interactions, can be evaluated by comparing the energy curves computed by using the adopted FF with the QM data obtained in this and in previous work.<sup>37</sup> In Figure 3, the quinhydrone interaction curves, previously computed for selected quinhydrone arrangements (see Supporting Information) at MP2mod and CCSD(T)@cbs levels, are compared to those obtained using OPLS parameters. It appears that OPLS gives rather accurate well depths for FF and SF arrangements but shows a tendency to overestimate the molecular steric hindrance. However, the agreement between FF and QM reference data can be improved by slightly

**Table 1. FF Intermolecular Parameters for Benzoquinone (Q) and Hydroquinone (H<sub>2</sub>Q)**

molecule	atom type	OPLS			RFF		
		q (e)	$\sigma$ (Å)	$\epsilon$ (kJ/mol)	q (e)	$\sigma$ (Å)	$\epsilon$ (kJ/mol)
Q	Ca	−0.115	3.55	0.293	−0.115	3.37	0.293
	C	0.470	3.75	0.499	0.470	3.37	0.499
	O	−0.470	3.07	0.711	−0.470	3.15	0.711
	Ha	0.115	2.42	0.293	0.115	2.35	0.293
H <sub>2</sub> Q	Ca	−0.115	3.55	0.293	−0.115	3.37	0.293
	Ha	0.115	2.42	0.293	0.115	2.35	0.293
	Cp	0.150	3.55	0.293	0.150	3.37	0.293
	Op	−0.585	2.96	0.877	−0.585	2.96	0.877
	Hp	0.435	0.00	0.000	0.435	0.00	0.000

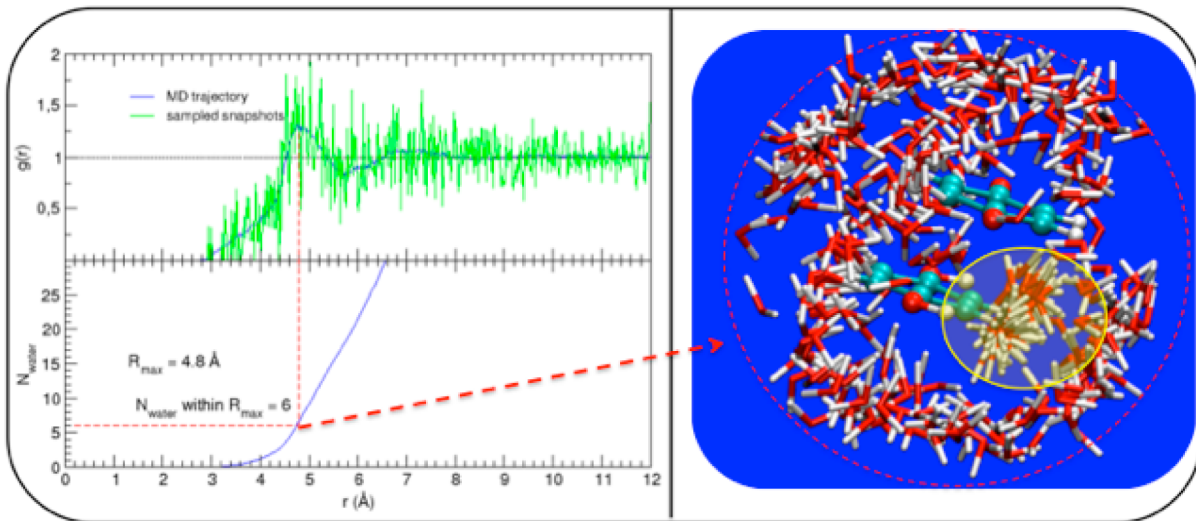


**Figure 4.** Top left:  $g(r)$  computed over the whole MD trajectory (blue) and over the sampled snapshots (green). Bottom left: Number ( $N_{\text{water}}$ ) of neighboring water molecules as a function of the center of mass distance. Right: superposition of the six closest water molecules (red dashed circle) extracted from the sampled snapshots; yellow circle indicates the set of H-bonded pairs.

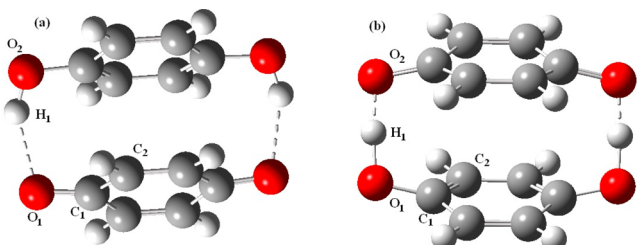


**Figure 5.** Optimized structures in vacuo. (a) quinhydrone,  $[\text{H}_2\text{Q}\cdots\text{Q}]$ ; (b) quinhydrone dianionic form,  $[\text{H}_2\text{Q}^{\cdot-}\cdots\text{Q}^{2-}]$ .

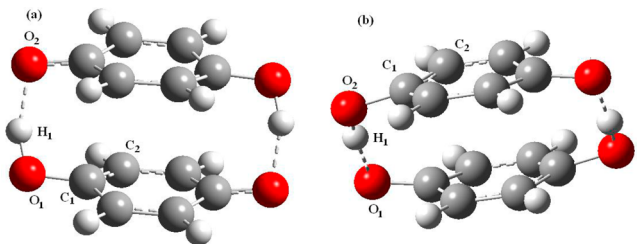


**Figure 6.** Optimized structures in vacuo. (a) semiquinone dimer,  $[\text{HQ}\cdots\text{HQ}]$ ; (b) hydroquinone ion complex,  $[\text{HQ}^{\cdot-}\cdots\text{HQ}^-]$ .

decreasing the LJ  $\sigma$  parameters for selected atom types. The results of such a refined FF (RFF) are also reported in Figure 3,

whereas all parameters of both original OPLS and RFF are reported in Table 1.

A final check can be performed verifying that the refinement accomplished on quinhydrone parameters does not alter the accuracy of the Q/H<sub>2</sub>O and H<sub>2</sub>Q/H<sub>2</sub>O interactions. As it appears from Figure 2, both OPLS and RFF are rather similar and close enough to QM data to reliably represent the hydrated quinhydrone system, although the accuracy is slightly worse than for the aromatic dimers. Therefore, the RFF parameters will be adopted for the intermolecular description in the MD simulations. Finally, as mentioned above, the intramolecular part of the FF for both benzoquinone and hydroquinone monomers has been derived by the JOYCE program.<sup>57,58</sup> Details on the parametrization procedure and its validation can be found in the Supporting Information.

**Solvation Structure.** The RFF (intermolecular) and the JOYCE derived (intramolecular) parameters were employed in MD simulations of the hydrated quinhydrone complex. As already mentioned, 10 ns runs were performed at 298 K and 1 atm on a system consisting in one quinhydrone complex Q/H<sub>2</sub>Q and almost 2000 water molecules. To estimate the number of water molecules surrounding the complex at a distance  $r$  ( $N_{\text{water}}(r)$ ), the  $g(r)$  between the centers of mass of quinhydrone and the surrounding water molecules was integrated from 0 up to 12 Å, as shown in Figure 4. A small number of frames was also randomly selected, to be used as starting point for QM geometry optimization.

**Table 2.** Energy Difference (kJ/mol), Atom–Atom Distances (Å), and Angles (degrees) of the Stable Structures of the  $[\text{H}_2\text{Q}\cdots\text{Q}]$  and  $[\text{HQ}^{\cdot-}\cdots\text{HQ}]$  Complexes (Figures 5a and 6a)<sup>a</sup>

	$[\text{H}_2\text{Q}\cdots\text{Q}]$				$[\text{HQ}^{\cdot-}\cdots\text{HQ}]$			
	vacuum	wat	ACE	DMSO	vacuum	wat	ACE	DMSO
$\Delta E$	0	-24.9	-24.3	-24.5	28.4	3.3	3.9	3.7
O <sub>1</sub> –H <sub>1</sub>	1.87	1.92	1.92	1.92	1.05	1.05	1.05	1.05
H <sub>1</sub> –O <sub>2</sub>	1.00	1.00	1.00	1.00	1.56	1.57	1.57	1.57
O <sub>1</sub> –H <sub>1</sub> –O <sub>2</sub>	151.2	148.5	148.7	148.7	157.3	156.8	156.8	156.8
H <sub>1</sub> –O <sub>1</sub> –C <sub>1</sub> –C <sub>2</sub>	-51.8	-49.2	-49.4	-49.37	-57.4	-57.3	-47.3	-47.3

<sup>a</sup>Wat, ACE, and DMSO indicate PCM calculations (wat = water, ACE = acetonitrile, and DMSO = dimethyl sulfoxide) The energy is referred to the optimized structure of  $[\text{H}_2\text{Q}\cdots\text{Q}]$  in vacuum.

Table 3.  $[\text{H}_2\text{Q}\cdots\text{Q}^{2-}]$  and  $[\text{HQ}^-\cdots\text{HQ}^-]$  Complexes<sup>a</sup> of Figures 5b and 6b

	$[\text{H}_2\text{Q}\cdots\text{Q}^{2-}]$				$[\text{HQ}^-\cdots\text{HQ}^-]$			
	vacuum	wat	ACE	DMSO	vacuum	wat	ACE	DMSO
$\Delta E$ (kJ/mol)	13.4	-688.5	-677.9	-682.2	0	-697.0	-686.5	-690.7
$\text{O}_1\text{-H}_1$	1.18	1.12	1.12	1.12	1.64	1.58	1.58	1.58
$\text{H}_1\text{-O}_2$	1.31	1.41	1.40	1.41	1.05	1.05	1.05	1.06
$\text{O}_1\text{-H}_1\text{-O}_2$	175.9	175.7	175.7	175.7	174.3	175.0	174.9	175.0
$\text{H}_1\text{-O}_1\text{-C}_1\text{-C}_2$	-51.7	-53.3	-53.2	-53.6	-54.6	-55.5	-55.4	-55.4

<sup>a</sup>See Table 2 for measurements and abbreviations.

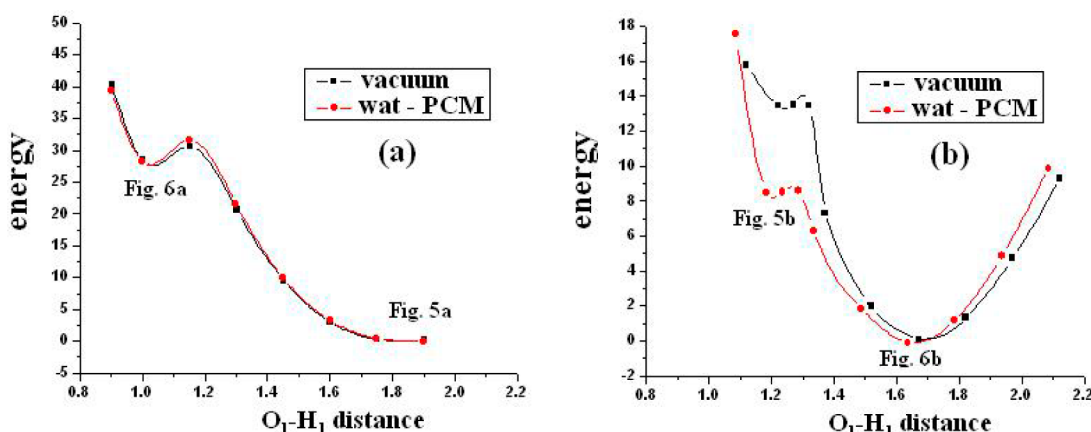


Figure 7. Potential energy curves (with and without water solvation by PCM) of the movement of the hydrogen atom in H-bridge. Part (a) neutral dimers; (b) dianionic dimers. At the minima, the figure of the corresponding structure is indicated. Distances are in Å and energy in kJ/mol. The numbering of the atoms is referred to in Figures 5 and 6.

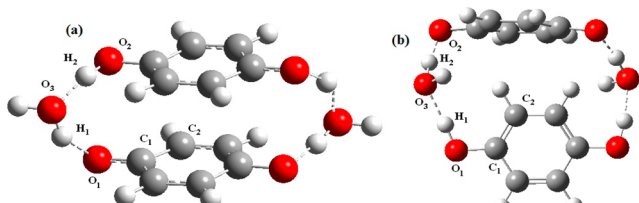


Figure 8. Optimized structures in vacuo. (a)  $[\text{H}_2\text{Q}\cdots\text{Q}] + 2\text{H}_2\text{O}$  complex ; (b)  $[\text{H}_2\text{Q}\cdots\text{Q}^{2-}] + 2\text{H}_2\text{O}$  complex.

From the top left panel of Figure 4, it is evident that, although noisy, the less averaged pcf represents well the distribution of solvent molecules achieved during the whole MD run. The most probable occurrence of a neighboring water molecule is at  $\sim 4.8$  Å, as indicated from the first peak of the  $g(r)$ . At this distance,  $N_{\text{water}} = 6$ , and this number was taken as a preliminary guess for the minimum number of water molecules to be explicitly considered in the QM calculations. Thus, a configuration consisting in the quinhydron complex sur-

rounded by these six  $\text{H}_2\text{O}$  molecules was extracted from each of the randomly selected frames and used as starting point for QM optimization at MP2mod level. The examination of the final optimized structures suggested that the number of explicitly considered solvent molecules could be further reduced, to improve the computational efficiency. Indeed, some additional observations support this hypothesis and suggest that just two water molecules are sufficient to represent most of the solute–solvent quantum effects: (i) in the right panel of Figure 4 is displayed the superimposition of all the first six neighboring water molecules extracted from each sampled frame. From visual inspection of the resulting patterns, it appears that most of the considered solvent molecules show a random position and/or orientation, except those closest to the hydroquinone OH group (see evidenced yellow region), being possibly involved in a HB interaction; (ii) an HB analysis, performed over the whole trajectory revealed that the average number of HBs formed between the solvent and the quinhydron complex is 4, with a residence time of more than 1.5 ps; (iii) after QM

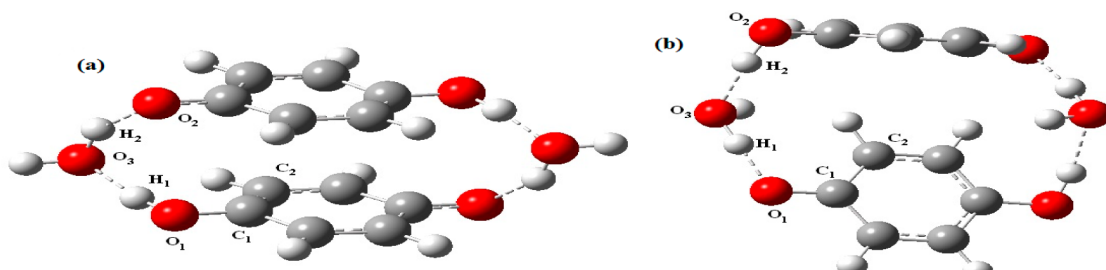
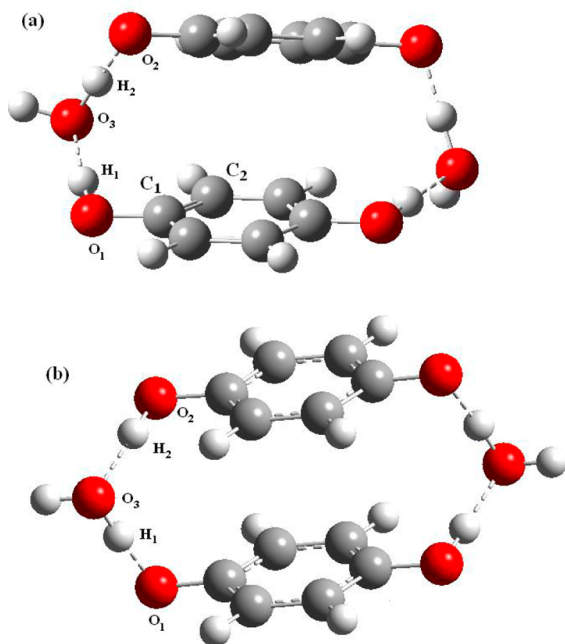


Figure 9. Optimized structures in vacuo. (a)  $[\text{HQ}\cdots\text{HQ}] + 2\text{H}_2\text{O}$  complex ; (b)  $[\text{HQ}^-\cdots\text{HQ}^-] + 2\text{H}_2\text{O}$  complex.



**Figure 10.** Optimized structures in PCM (water). (a) ( $[H_2Q \cdots Q]^{2-} + 2H_2O$ ) + water complex; (b) ( $[HQ \cdots HQ]^{2-} + 2H_2O$ ) + water complex.

optimization, among the six considered water molecules, only two of them are always found one on each side of the complex, connecting the two quinoid moieties through lateral H-bridges (see also Figures 8, 9, and 10).

**Stability of the Quinoid Complexes.** Several species should be taken into account to determine the stability of quinhydrone-like complexes: neutral ( $Q$ ,  $HQ$  or semiquinone,  $H_2Q$ ), monoanionic ( $HQ^-$ ), or dianionic ( $Q^{2-}$ ). All these monomers and the redox and/or dissociation equilibria of their interconversion are displayed in Scheme 1. Several different configurations can be obtained by placing two of the above-mentioned monomers in a stacked arrangement. Among the many possible combinations, we have focused our attention on the quinhydrone complex  $[H_2Q \cdots Q]$ , the semiquinone dimer  $[HQ \cdots HQ]$ , and their reduced complexes,  $[H_2Q \cdots Q^{2-}]$  and  $[HQ^- \cdots HQ^-]$ , respectively. We should underline that this notation with localized negative charges for the dianionic species is only symbolic and follows that of ref 35. This does

not necessarily imply that we are in the presence of a pure proton transfer between the two moieties.

In Figure 5 are displayed quinhydrone (panel (a),  $[H_2Q \cdots Q]$ ) and its dianionic form (panel (b),  $[H_2Q \cdots Q^{2-}]$ ), whereas in Figure 6 are shown the systems obtained by combining two semiquinones (panel (a),  $[HQ \cdots HQ]$ ) and hydroquinone ions (panel (b),  $[HQ^- \cdots HQ^-]$ ). As previously discussed, the four complexes were also optimized in protic and aprotic solvents, namely,  $H_2O$ , DMSO, and ACE, at the PCM level. The corresponding structures of the solvated systems are not reported because they are very similar to those obtained in vacuo. In the water case, the standard PCM description was also complemented with the addition of 2 explicit water molecules, that is the whole  $[H_2Q \cdots Q] + 2H_2O$ ,  $[HQ \cdots HQ] + 2H_2O$ ,  $[H_2Q \cdots Q^{2-}] + 2H_2O$  and  $[HQ^- \cdots HQ^-] + 2H_2O$  systems were embedded in the PCM water medium. This allows us to incorporate QM effects due to the participation of the water molecules to the formation of the complexes, taking into account a global polarization of the media. For the sake of clarity, this latter case will be separately discussed, after PCM and in vacuo results. All these structures were obtained through a complete geometry optimization at MP2mod level of theory.

In Table 2 are reported the energy and some geometrical data relevant to the possible HBs formed within the structures of Figure 5a and 6a. Similarly, in Table 3, those of Figure 5b and 6b are shown. It is important to notice that for each table, the two complexes therein described are connected by a hydrogen transfer reaction.

Some preliminary considerations can be made from the analysis and comparison of Figures 5 and 6 and Tables 2 and 3. First of all, as far as the neutral complexes are concerned (Figures 5a,b and Table 2), the most stable structure is quinhydrone  $[H_2Q \cdots Q]$ , whereas, between the charged ones, the reduced semiquinone dimer  $[HQ^- \cdots HQ^-]$  appears to be favored. This suggests that in the two-electron reduction process of quinhydrone, a one-proton transfer mechanism should occur. Next, regarding solvent effects, no significant differences were found between in vacuo and PCM calculations. In particular, in the comparison among the water and the aprotic solvents (acetonitrile and dimethyl sulfoxide), the changes of both structures and energies of the complexes are also not significant, at least at PCM level.

For the dianionic quinhydrone complex in vacuo (Figure 5b), it is evident that both hydrogen atoms involved in the HB are nearly equally shared by the two rings (~1.18 and 1.31 Å from the oxygen atoms), whereas for the neutral case and in the

**Table 4. Distances (Å), Angles (degrees), and Energy (kJ/mol) of the Stable Structures of the Four Complexes with Two Explicit Water Molecules<sup>a</sup>**

	$[H_2Q \cdots Q] + 2H_2O$		$[HQ \cdots HQ] + 2H_2O$		$[H_2Q \cdots Q^{2-}] + 2H_2O$		$[HQ^- \cdots HQ^-] + 2H_2O$	
	vacuum	wat	vacuum	wat	vacuum	wat	vacuum	wat
$\Delta E$ (kJ/mol)	0	-49.5	16.8	-24.1	11.8	-640.1	0	-643.6
$O_1-H_1$	1.79	1.76	1.02	1.03	1.03	1.03	1.74	1.72
$H_1-O_1-C_1-C_2$	-7.8	-7.7	-8.6	-8.0	1.5	-22.7	-112.8	-17.1
$H_1-O_3$	1.01	1.01	1.69	1.67	1.69	1.65	1.02	1.01
$O_1-H_1-O_3$	167.2	170.9	170.3	170.7	173.1	173.2	168.5	175.1
$O_3-H_2$	1.83	1.91	0.98	0.99	1.07	1.07	1.53	1.52
$H_2-O_2$	0.99	0.98	1.74	1.80	1.48	1.45	1.05	1.04
$O_3-H_2-O_2$	149.1	144.3	149.4	147.1	170.5	174.3	174.0	173.7

<sup>a</sup>The column named wat is related to embedding the complex with the two waters in a PCM cavity. O–H and H···O are, respectively, the covalent and hydrogen bond in a H-bridge, O–H–O the bond angle, and H–O–C–C a dihedral angle.

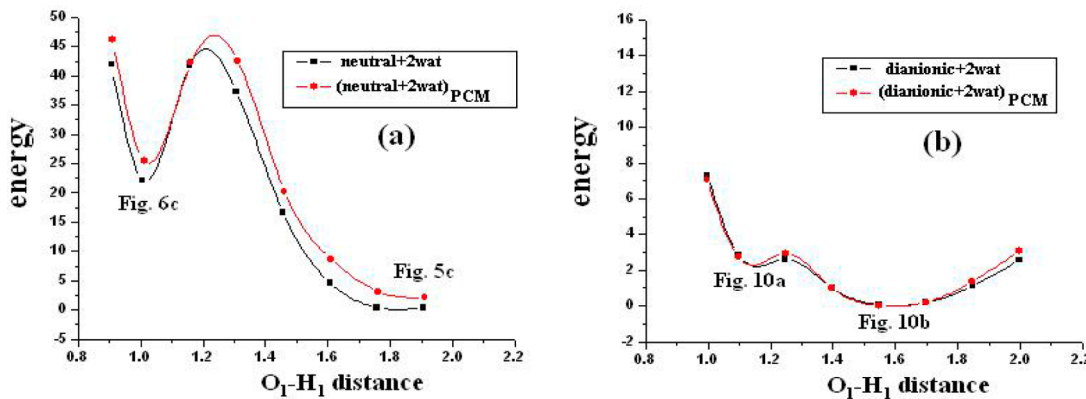


**Figure 11.** Potential energy curves of the movement of the hydrogen atom in H-bridge for the species with two explicit water molecules, with and without water adding solvation by PCM. Part (a) neutral dimers; (b) dianionic dimers. At the minima, the figure of the corresponding structure is indicated. Distances are in Å and energy in kJ/mol.

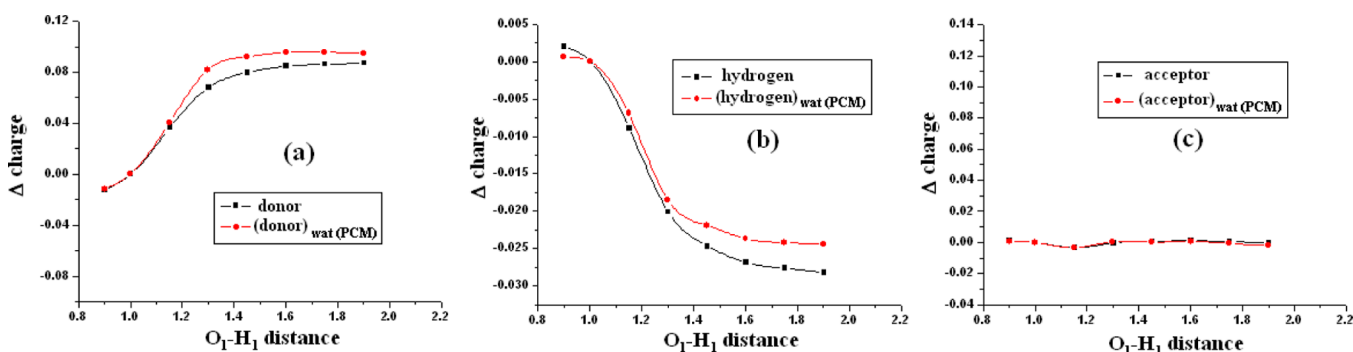


**Figure 12.** Natural atomic charges of the atoms of the H-bridge during the movement of the hydrogen atom from the donor to the acceptor (distance is in Å). The system is the neutral complex in vacuum and in water by PCM.

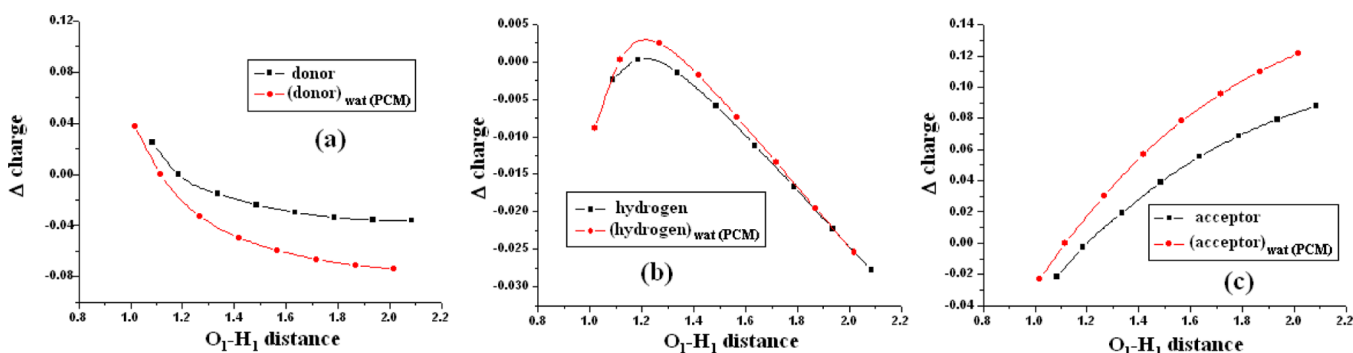


**Figure 13.** As in Figure 12, but for the dianionic system in vacuum and in water by PCM.

solvated structures each H atom belongs to a well-defined ring. All O—H···O H-bridges are almost linear. It may be worth noticing that, as in our previous paper,<sup>37</sup> the hydrogen atoms are out-of plane of the benzene structure in the neutral dimers.

The energy difference between the equilibrium structures of the two complexes ( $[H_2Q \cdots Q^{2-}]$  and  $[HQ^- \cdots HQ^-]$ ) is around 13 kJ/mol (see Table 3), a value much smaller than that of ref 35 (~80 kJ/mol), and much more compatible with an effective thermal interconversion near room temperature.

**Proton Transfer.** A better comparison between experimental and theoretical results can be performed in terms of the energy variations issuing from geometry optimizations at fixed positions of the hydrogen atom involved in the intermolecular bridge.

In panel (a) of Figure 7, where the movement of the H<sub>1</sub> atom in the O<sub>1</sub>—H<sub>1</sub>—O<sub>2</sub> H-bridge (for the numbering of the atoms see Figures 5 and 6) was investigated, the MEP for the  $[H_2Q \cdots Q] \rightleftharpoons [HQ \cdots HQ]$  proton transfer is shown, with and without the inclusion of solvent effects by PCM. In panel (b) is reported the MEP for the  $[H_2Q \cdots Q^{2-}] \rightleftharpoons [HQ^- \cdots HQ^-]$  proton transfer. Because only energy differences are relevant, in both panels (a) and (b), the PCM curves have been shifted in energy by 24.9 and 697 kJ/mol, respectively, so that the zero in energy corresponds to the most stable species:  $[H_2Q \cdots Q]$  in panel (a) and  $[HQ^- \cdots HQ^-]$  in panel (b).

Panel (a) shows that the  $[HQ \cdots HQ]$  complex is 28.4 kJ/mol higher than the more stable  $[H_2Q \cdots Q]$  dimer and the interconversion barrier toward quinhydrone is very small (2.2 kJ/mol). The corresponding paths with the other two solvents

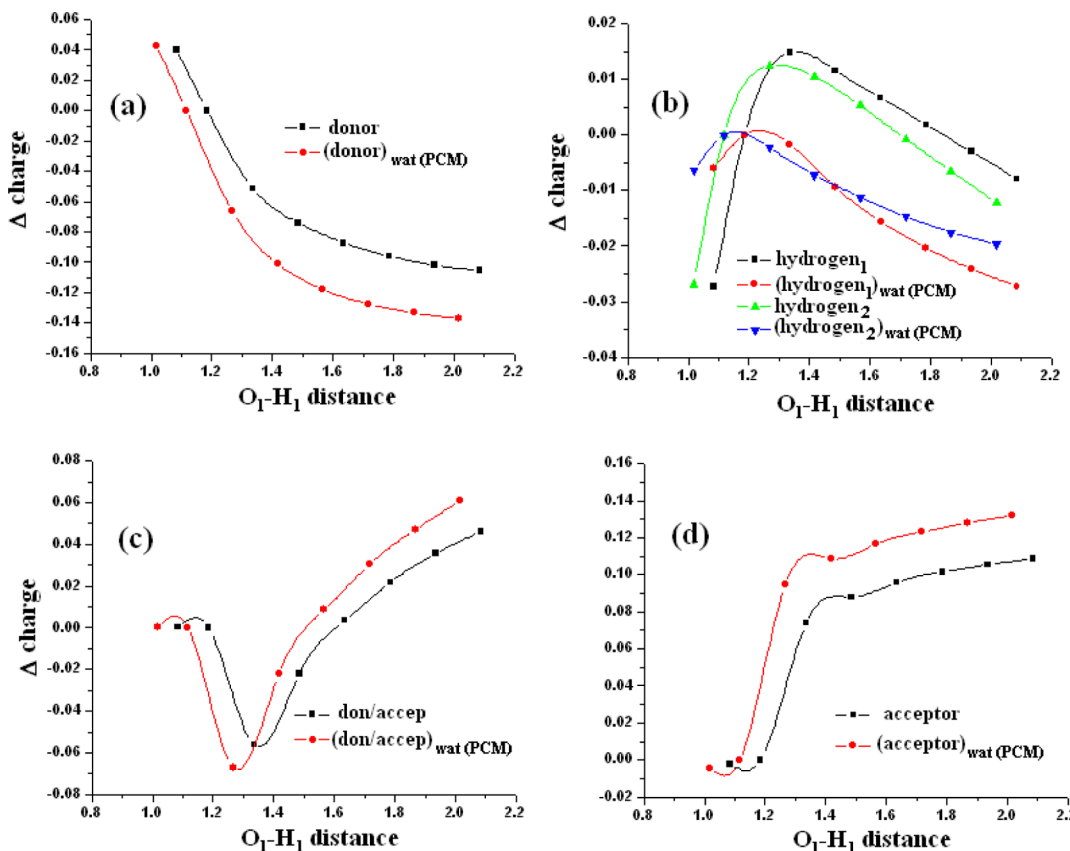


**Figure 14.** Natural atomic charges of the atoms of the two H-bridge ( $O_1-H_1\cdots O_3$  and  $O_3-H_2\cdots O_2$ ) during the movement of the hydrogen atom from the donor to the water molecule (distances in angstrom). The system is the neutral complex with two explicit water molecules, in vacuo and with PCM.

considered in this paper, ACE and DMSO, have not been reported in the figure, because they are practically indistinguishable from the water case. Inclusion of solvent effects by the PCM does not change substantially the shape of the potential energy curves, with the exception of the barrier, that increases from 2.2 to 3.5 kJ/mol. In panel (b), one can see a marked decrease of the energy gap between the two species  $[H_2Q\cdots Q^{2-}]$  and  $[HQ^-\cdots HQ^-]$ , as well as a very strong decrease of the barrier. The inclusion of solvent effects at the PCM level gives rise to a further decrease of the gap, as one would expect for charged species. As already mentioned, the authors of ref 35 have considered the possibility of a fast interchange between these two dimeric structures, as suggested by the experimental studies, but they found a barrier of more than 80 kJ mol<sup>-1</sup>, which does not justify the thermal interchange at 298 K. The data of Tables 2 and 3 and Figure 7 suggest a very small barrier for the interchange and hence are in good agreement with the experimental results.<sup>35,36</sup>

**Proton Transfer in Protic Solvents.** The different solvents considered so far showed a very similar behavior at the PCM level. However, whenever a protic solvent is considered, the possible formation of intermolecular HBs with the species under study should be taken into account. For this reason, two explicit water molecules have been included, together with PCM, to model aqueous solutions. The final optimized structures of neutral and dianionic complexes are shown in Figures 8 (panel (a) for  $[H_2Q\cdots Q] + 2H_2O$  and panel (b) ( $[H_2Q\cdots Q^{2-}] + 2H_2O$ ) in Figures 9, (panels (a) and (b)

for  $[HQ\cdots HQ] + 2H_2O$  and  $[HQ^-\cdots HQ^-] + 2H_2O$ , respectively).

By comparing Figures 8 and 9 with Figures 5 and 6, it is apparent that water molecules act as further linkers in the dimers formed by the two organic molecules.

It is evident from panel (b) of Figures 8 and 9 that the dianionic complexes with two explicit water molecules have a different structure from the others, with the two rings almost perpendicular to each other. A more reliable description could be achieved if the bulk solvent effect on the explicitly hydrated complexes is added through a PCM description. In this case the  $[H_2Q\cdots Q^{2-}] + 2H_2O$  and  $[HQ^-\cdots HQ^-] + 2H_2O$  complexes assume an arrangement similar to the ones of Figures 5b and 6b with a water molecule interposed at each side of the complex. Such structures are reported in Figure 10, although the relevant geometric and energetic data are summarized in Table 4.

Due to the insertion of water molecules, the separation of the two rings increases. The  $O-H\cdots O$  group deviates from linearity, and in the neutral dimer the HB is smaller than the others; the addition of the continuum water solvent decrease it even more.

By comparing the energetic data of Table 4 with those of Tables 2, 3, it is apparent that the relative stability of the complexes involved in proton transfer equilibria is the same, so that these last data confirm that the two-electron reduction implies a proton transfer.

In Figure 11, the MEP for the relaxed hydrogen transfer between the neutral, (a), and dianionic, (b), species are

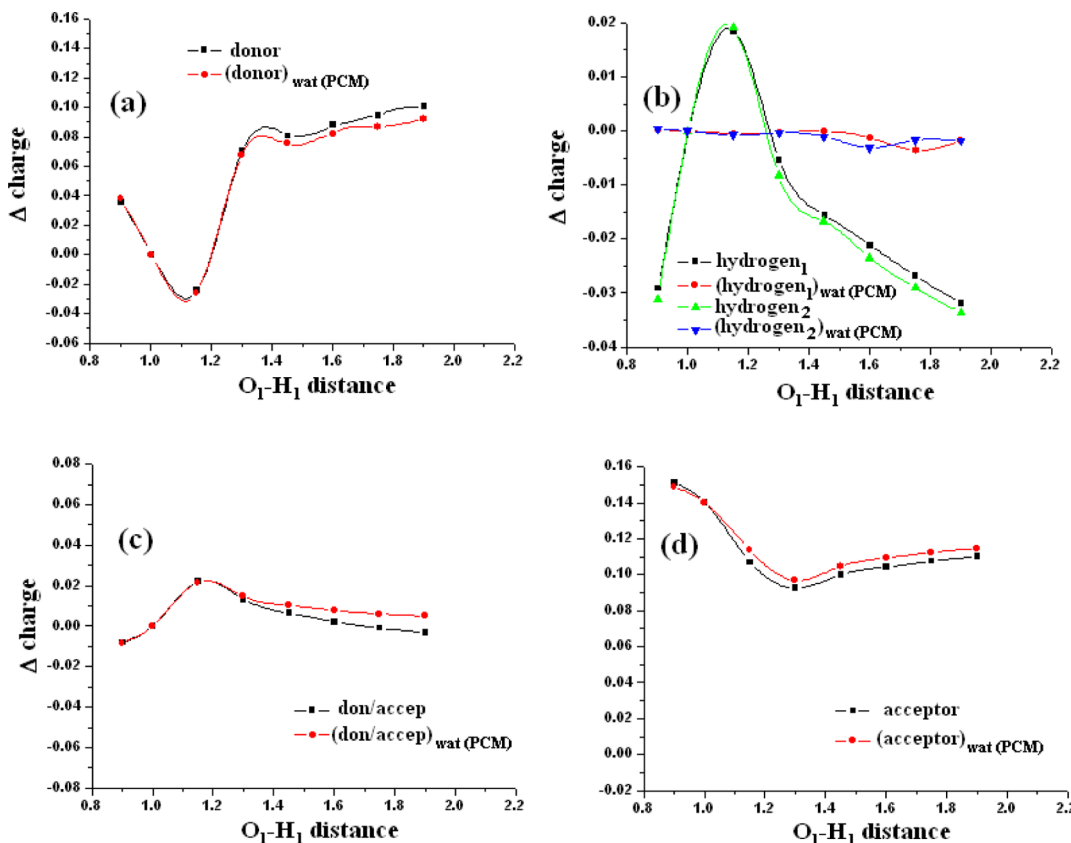


Figure 15. As in Figure 14, but for the dianionic system in vacuo and with PCM.

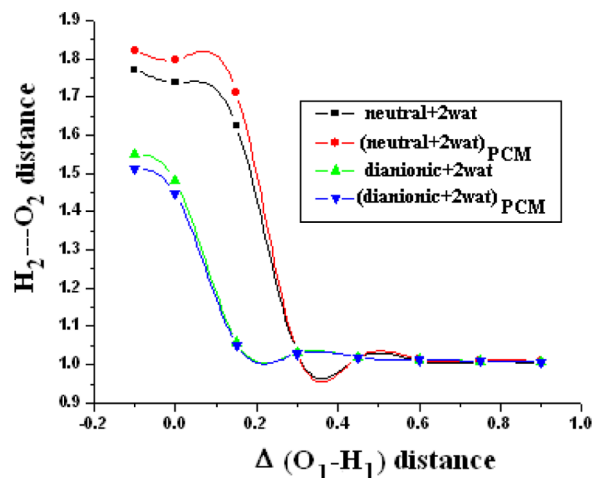


Figure 16. Length of the hydrogen bond from the water to the acceptor atom during the movement of the hydrogen atom in the H-bridge between the donor atom and the water molecule ( $\Delta$  distance is the difference from the equilibrium value). All distances are in Å.

reported. The two minima correspond to the energies reported in Table 4. When including two explicit water molecules, the  $[\text{HQ}\cdots\text{HQ}]\text{+2H}_2\text{O}$  complex is 21.1 and 25.4 kJ/mol higher in energy than the  $[\text{H}_2\text{Q}\cdots\text{Q}]\text{+2H}_2\text{O}$  system, and the corresponding barriers are 19.7 and 16.8 kJ/mol, without and with the PCM description of bulk solvent, respectively. Therefore, the effect of the PCM is an increase of the energy difference and a decrease of the barrier. In the case of dianionic species, the semiquinone-like system is the most stable, but the barrier for the hydrogen transfer is higher with respect to Figure 7.

### Concerted Mechanisms for Electron and Proton Transfer.

As a final step, in order to better define the nature of the transferred species (i.e., a proton or an H atom), we calculated the natural charges of the atoms involved in the H-bridge along the transfer path. The charge differences with respect to the equilibrium values as a function of the O–H distances of Figure 7, in vacuo and in water by PCM, are shown in Figures 12 and 13 for the neutral and for the dianionic complexes, respectively.

In Figure 12, we can see that the charges of the hydrogen and the donor and acceptor oxygens do not show significant variations. The acceptor charge is nearly constant, whereas the small decrease of charge of the donor, going from quinhydrone to semiquinone is found as an increase of the charge of the hydrogen. This means that the hydrogen remains with the fraction of electron of the equilibrium structure during the passage from the donor oxygen to the acceptor one, and this situation is only slightly modified when the water solvent in the PCM approach is included (Figure 9). In the figures, we do not show the atomic charges in the other two solvents considered in this paper (acetonitrile and dimethyl sulfoxide), because the results are practically indistinguishable from those in water. In spite of possible limitations of the PCM, the very close PES and charge distribution in the process of transfer, further support is given to the hypothesis that we are in the presence of a hydrogen atom rather than a proton transfer.

We can notice also a slight different behavior of neutral and dianionic complex. In fact, in the case of the anionic species, the small charge variation of the donor is then found on the acceptor oxygen.

This last effect is also found in the complexes with two explicit water molecules, as shown in the (a) and (d) panels of

Figures 14 and 15, where the charge variations along the transfer path for the species with two explicit water molecules are reported. In any case, the variations in the atomic charges are rather small (tenths of unit charge), and therefore, also for the dianionic species, we are in the presence of a hydrogen atom transfer rather than a proton transfer, in agreement with the conclusions drawn from experimental results in ref 35.

Although charge variations are still limited, the role of explicit water molecules is quite apparent because they allow a sort of concerted mechanism in which the hydrogen transfer may occur involving two different atoms; that is, as H<sub>1</sub> get closer to O<sub>3</sub> in Figure 10, H<sub>2</sub> get closer to O<sub>2</sub>.

In order to study this possibility, in Figure 16 we have reported the variations of the length of the hydrogen bond between the water and the acceptor atom, when the hydrogen moves from the donor oxygen to the water molecule. In the figure, it is evident that the two hydrogen atoms move in a concerted way, with the H<sub>2</sub>–O<sub>2</sub> distance decreasing as H<sub>1</sub>–O<sub>1</sub> increases. However, no correlation has been found between the movement of these two hydrogen atoms and the two hydrogens pertaining to the H-bridge on the other side of the complex. Indeed, these atoms do not show any synchronic significant displacement.

## CONCLUSIONS

In this paper, we have studied complexes made by stable species derived by 1,4-benzoquinone and hydroquinone with the aim to investigate their proton or hydrogen atom transfer equilibria:



From a computational point of view, we are able to propose and validate an effective yet reliable MP2 model able, by means of proper modification of polarization functions, to approach the accuracy of very reliable yet computationally prohibitive CCSD(T) computations with complete basis set extrapolation. Next, bulk solvent effects were taken into account by the PCM, and when needed, specific interactions in the cybotactic region were properly described by adding a few explicit solvent molecules. In parallel, parametrization of a reliable force field has allowed preliminary investigations of solvent structures by means of Molecular Dynamics simulations. After calibration and validation of the computational model, we have undertaken a systematic evaluation of the structures and relative stabilities of different dimers together with an unbiased analysis of the nature (cation or neutral atom) of the bridging hydrogens.

For neutral systems, we have found that the quinhydrone [Q···H<sub>2</sub>Q] is by far the most stable complex (~25 kJ/mol). For the anionic systems, the [HQ<sup>-</sup>···HQ<sup>-</sup>] dimer appears to be the preferred form, and the energy difference with the [Q<sup>2-</sup>···H<sub>2</sub>Q] complex is roughly 8 and 13 kJ/mol with or without PCM, respectively.

A minimum energy path for the proton/hydrogen transfer reaction has then been obtained in order to evaluate the activation energy for the two equilibria. This depends on solvation, but quite similar mechanisms are observed in different solvents. Investigation of the charge distribution confirms then that the systems undergo a hydrogen atom transfer. This also holds when water molecules are explicitly considered. In this case, the relative stability of the species in the two equilibria is not altered, whereas the barriers are seen to change. A major variation is seen for the neutral species, whereas for the ionic species, the change in the barrier height

(from 8 to 3 kJ/mol) is in an even better agreement with the experimental detection of both Q<sup>2-</sup> and HQ<sup>-</sup> species, with respect to the PCM description.

From a specific point of view, the most interesting outcome of our study is the demonstration of similar stabilities of [QH<sup>-</sup>···QH<sup>-</sup>] and [Q<sup>2-</sup>···H<sub>2</sub>Q] complexes, which are furthermore connected by a low activation energy path: this is at variance with a previous computational study and restores the agreement with experiments pointing out an effective thermal interconversion between the two complexes.

In more general terms, the proposed approach should be fast and reliable enough to allow semiquantitative analysis of different reaction mechanisms for fairly large species both in vacuum and in condensed phases.

## ASSOCIATED CONTENT

### Supporting Information

Four figures are reported in the SI detailed as follows: Dimer arrangements for the quinhydrone complex considered for the validation of the intermolecular RFF; Vibrational frequencies for Q and H<sub>2</sub>Q monomers computed at QM level and with the JOYCE parametrized FF; Torsional energy curves of the rotation around the C–O bond in H<sub>2</sub>Q obtained at QM level and with the JOYCE parametrized FF; Test calculation on [HQ<sup>-</sup>···HQ<sup>-</sup>] performed at MP2mod and CCSD(T)/aug-cc-pVQZ level. This material is available free of charge via the Internet at <http://pubs.acs.org>.

## AUTHOR INFORMATION

### Corresponding Author

\*E-mail: villani@pi.iccom.cnr.it.

### Funding

The Italian Ministry of Instruction, University and Research (MIUR) is acknowledged for financial funding through the PRIN 2010-11 project (PROxi).

### Notes

The authors declare no competing financial interest.

## REFERENCES

- Cherney, M. M.; Zhang, Y.; James, M. N. G.; Weiner, J. H. Structure–Activity Characterization of Sulfide: Quinone Oxidoreductase Variants. *J. Struct. Biol.* **2012**, *178*, 319–328.
- Furman, N. H.; Stone, K. G. A Polarographic Study of Certain Anthraquinones. *J. Am. Chem. Soc.* **1948**, *70*, 3055–3061.
- Matsuura, K.; Packham, N. K.; Mueller, P.; Dutton, P. L. The Recognition and Redox Properties of a Component, Possibly a Quinone, Which Determines Electron Transfer Rate in Ubiquinone-Cytochrome C Oxidoreductase of Mitochondria. *FEBS Lett.* **1981**, *131*, 17–22.
- Austen, D. E. G.; Given, P. H.; Ingram, D. J. E.; Peover, M. E. Electron Resonance Study of the Radicals Produced by Controlled Potential Electrolysis of Aromatic Substances. *Nature* **1958**, *182*, 1784–1786.
- Gupta, N.; Linschitz, H. Hydrogen-Bonding and Protonation Effects in Electrochemistry of Quinones in Aprotic Solvents. *J. Am. Chem. Soc.* **1997**, *119*, 6384–6391.
- Russel, C.; Jaenicke, W. Heterogeneous Electron Exchange of Quinones in Aprotic Solvents. *Z. Phys. Chem.* **1984**, *139*, 97–112.
- Russel, C.; Jaenicke, W. Heterogeneous Electron Exchange of Quinones in Aprotic Solvents: Part III. The Second Reduction Step of P-Benzoylquinone and Its Dependence on the Supporting Electrolyte. *J. Electroanal. Chem.* **1986**, *199*, 139–151.
- Uno, B.; Okumura, N.; Goto, M.; Kano, K. n–σ Charge-Transfer Interaction and Molecular and Electronic Structural Properties in the

- Hydrogen-Bonding Systems Consisting of P-Quinone Dianions and Methyl Alcohol. *J. Org. Chem.* **2000**, *65*, 1448–1455.
- (9) Wawzonek, S.; Berkey, R.; Blaha, E. W.; Runner, M. E. Polarographic Studies in Acetonitrile and Dimethylformamide: III. Behavior of Quinones and Hydroquinones. *J. Electrochem. Soc.* **1956**, *103*, 456–459.
- (10) Bautista-Martínez, J. A.; González, I.; Aguilar-Martínez, M. Influence of Acidity Level in Acetonitrile on Hammett–Zuman Type Correlations on the Reduction of A-Hydroxyquinones. *Electrochim. Acta* **2003**, *48*, 4239–4244.
- (11) Chambers, J. Q. Electrochemistry of Quinones. In *The Chemistry of Quinonoid Compounds*; Patai, S., Rappoport, Z., Eds.; John Wiley and Sons, Ltd.: London, United Kingdom, 1988; Vol. II, 719–758.
- (12) Gómez, M.; González, F. J.; González, I. A Model for Characterization of Successive Hydrogen Bonding Interactions with Electrochemically Generated Charged Species. The Quinone Electro-reduction in the Presence of Donor Protons. *Electroanalysis* **2003**, *15*, 635–645.
- (13) Gómez, M.; González, F. J.; González, I. Effect of Host and Guest Structures on Hydrogen Bonding Association: Influence on Stoichiometry and Equilibrium Constants. *J. Electrochem. Soc.* **2003**, *150*, E527–E534.
- (14) Gómez, M.; González, I.; González, F. J.; Vargas, R.; Garza, J. The Association of Neutral Systems Linked by Hydrogen Bond Interactions: A Quantitative Electrochemical Approach. *Electrochim. Commun.* **2003**, *5*, 12–15.
- (15) Hodnett, E. M.; Wongwiechintana, C.; Dunn, W. J., III; Marrs, P. Substituted 1,4-Naphthoquinones Vs. The Ascitic Sarcoma 180 of Mice. *Med. Chem. Lett.* **1983**, *26*, 570–574.
- (16) Saito, K.; Rutherford, A. W.; Ishikita, H. Mechanism of Proton-Coupled Quinone Reduction in Photosystem II. *Proc. Natl. Acad. Sci. U.S.A.* **2013**, *110*, 954–959.
- (17) Aguilar-Martínez, M.; Macías-Ruvalcaba, N. A.; Bautista-Martínez, J. A.; Gómez, M.; González, F. J.; González, I. Review: Hydrogen Bond and Protonation as Modifying Factors of the Quinone Reactivity. *Curr. Org. Chem.* **2004**, *8*, 1721–1738.
- (18) Weinberg, D. R.; Gagliardi, C. J.; Hull, J. F.; Murphy, C. F.; Kent, C. A.; Westlake, B. C.; Paul, A.; Ess, D. H.; McCafferty, D. G.; Meyer, T. J. Proton-Coupled Electron Transfer. *Chem. Rev.* **2012**, *112*, 4016–4093.
- (19) Pang, X. F. Properties of Proton Transfer in Hydrogen-Bonded Systems and Its Experimental Evidences and Applications in Biology. *Prog. Biophys. Mol. Biol.* **2013**, *112*, 1–32.
- (20) Hang, M.; Huynh, V.; Meyer, T. Proton-Coupled Electron Transfer. *Chem. Rev.* **2007**, *107*, 5004–5064.
- (21) Cukier, R. I.; Nocera, D. G. Proton-Coupled Electron Transfer. *Annu. Rev. Phys. Chem.* **1998**, *49*, 337–369.
- (22) Decornez, H.; Hammes-Schiffer, S. Model Proton-Coupled Electron Transfer Reactions in Solution: Predictions of Rates, Mechanisms, and Kinetic Isotope Effects. *J. Phys. Chem. A* **2000**, *104*, 9370–9384.
- (23) Pause, L.; Robert, M.; Savéant, J. M. Stepwise and Concerted Pathways in Photoinduced and Thermal Electron-Transfer/Bond-Breaking Reactions. Experimental Illustration of Similarities and Contrasts. *J. Am. Chem. Soc.* **2001**, *123*, 4886–4893.
- (24) Fecenko, C. J.; Thorp, H. H.; Meyer, T. J. The Role of Free Energy Change in Coupled Electron–Proton Transfer. *J. Am. Chem. Soc.* **2007**, *129*, 15098–15099.
- (25) Gray, H. B.; Winkler, J. R. Long-Range Electron Transfer. *Proc. Natl. Acad. Sci. U.S.A.* **2005**, *102*, 3534–3539.
- (26) Duncan Lyngdoh, R. H.; Schaefer, H. F., III Elementary Lesions in DNA Subunits: Electron, Hydrogen Atom, Proton, and Hydride Transfers. *Acc. Chem. Res.* **2009**, *42*, 563–572.
- (27) Gu, J.; Xie, Y.; Schaefer, H. F., III Electron Attachment Induced Proton Transfer in a DNA Nucleoside Pair: 2'-Deoxyguanosine-2'-Deoxycytidine. *J. Chem. Phys.* **2007**, *127*, 155107.
- (28) Zhang, J. D.; Chen, Z.; Schaefer, H. F., III Electron Attachment to the Hydrogenated Watson–Crick Guanine Cytosine Base Pair (GC +H): Conventional and Proton-Transferred Structures. *J. Phys. Chem. A* **2008**, *112*, 6217–6226.
- (29) Villani, G. Theoretical Investigation of Hydrogen Atom Transfer in the Adenine–Thymine Base Pair and Its Coupling with the Electronic Rearrangement. Concerted Vs. Stepwise Mechanism. *Phys. Chem. Chem. Phys.* **2010**, *12*, 2664–2669.
- (30) Villani, G. Theoretical Investigation of Hydrogen Atom Transfer in the Cytosine–Guanine Base Pair and Its Coupling with Electronic Rearrangement. Concerted Vs. Stepwise Mechanism. *J. Phys. Chem. B* **2010**, *114*, 9653–9662.
- (31) Villani, G. Theoretical Investigation of the Hydrogen Atom Transfer in the Hydrated A-T Base Pair. *Chem. Phys.* **2012**, *394*, 9–16.
- (32) Villani, G. Theoretical Investigation of Hydrogen Atom Transfer in the Hydrated C-G Base Pair. *Mol. Phys.* **2013**, *111*, 201–214.
- (33) Ma, W.; Long, Y.-T. Quinone/Hydroquinone-Functionalized Biointerfaces for Biological Applications from the Macro- to Nano-Scale. *Chem. Soc. Rev.* **2014**, *43*, 30–41.
- (34) Astudillo, P. D.; Tiburcio, J.; González, F. J. The Role of Acids and Bases on the Electrochemical Oxidation of Hydroquinone: Hydrogen Bonding Interactions in Acetonitrile. *J. Electroanal. Chem.* **2007**, *604*, 57–64.
- (35) Astudillo, P. D.; Valencia, D. P.; González-Fuentes, M. A.; Diaz-Sánchez, B. R.; Frontana, C.; González, F. J. Electrochemical and Chemical Formation of a Low-Barrier Proton Transfer Complex between the Quinone Dianion and Hydroquinone. *Electrochim. Acta* **2012**, *81*, 197–204.
- (36) Salas, M.; Gómez, M.; González, F. J.; Gordillo, B. Electrochemical Reduction of 1,4-Benzooquinone. Interaction with Alkylated Thymine and Adenine Nucleobases. *J. Electroanal. Chem.* **2003**, *543*, 73–81.
- (37) Barone, V.; Cacelli, I.; Crescenzi, O.; D’Ischia, M.; Ferretti, A.; Prampolini, G.; Villani, G. Unraveling the Interplay of Different Contributions to the Stability of the Quinhydrone Dimer. *RSC Adv.* **2014**, *4*, 876–885.
- (38) Řezáč, J.; Hobza, P. Describing Noncovalent Interactions Beyond the Common Approximations: How Accurate Is the “Gold Standard,” Ccsd(T) at the Complete Basis Set Limit? *J. Chem. Theory Comput.* **2013**, *9*, 2151–2155.
- (39) González Moa, M. J.; Mandado, M.; Mosquera, R. A. A Computational Study on the Stacking Interaction in Quinhydrone. *J. Phys. Chem. A* **2007**, *111*, 1998–2001.
- (40) Grimme, S. Density Functional Theory with London Dispersion Corrections. *Wiley Interdisciplinary Reviews: Computational Molecular Science* **2011**, *1*, 211–228.
- (41) Frisch, M. J.; Trucks, G. W.; Schlegel, H. B.; Scuseria, G. E.; Robb, M. A.; Cheeseman, J. R.; Scalmani, G.; Barone, V.; Mennucci, B.; Petersson, G. A.; Nakatsuji, H.; Caricato, M.; Li, X.; Hratchian, H. P.; Izmaylov, A. F.; Bloino, J.; Zheng, G.; Sonnenberg, J. L.; Hada, M.; Ehara, M.; Toyota, K.; Fukuda, R.; Hasegawa, J.; Ishida, M.; Nakajima, T.; Honda, Y.; Kitao, O.; Nakai, H.; Vreven, T.; Montgomery, J. A., Jr.; Peralta, J. E.; Ogliaro, F.; Bearpark, M.; Heyd, J. J.; Brothers, E.; Kudin, K. N.; Staroverov, V. N.; Kobayashi, R.; Normand, J.; Raghavachari, K.; Rendell, A.; Burant, J. C.; Iyengar, S. S.; Tomasi, J.; Cossi, M.; Rega, N.; Millam, M. J.; Klene, M.; Knox, J. E.; Cross, J. B.; Bakken, V.; Adamo, C.; Jaramillo, J.; Gomperts, R.; Stratmann, R. E.; Yazyev, O.; Austin, A. J.; Cammi, R.; Pomelli, C.; Ochterski, J. W.; Martin, R. L.; Morokuma, K.; Zakrzewski, V. G.; Voth, G. A.; Salvador, P.; Dannenberg, J. J.; Dapprich, S.; Daniels, A. D.; Farkas, Ö.; Foresman, J. B.; Ortiz, J. V.; Ciosowski, J.; Fox, D. J. *Gaussian09*, revision D.01; Gaussian, Inc.: Wallingford, CT, 2009.
- (42) Prampolini, G.; Monti, S.; De Mitri, N.; Barone, V. Evidences of Long Lived Cages in Functionalized Polymers: Effects on Chromophore Dynamic and Spectroscopic Properties. *Chem. Phys. Lett.* **2014**, *601*, 134–138.
- (43) Tomasi, J.; Mennucci, B.; Cammi, R. Quantum Mechanical Continuum Solvation Models. *Chem. Rev.* **2005**, *105*, 2999–3196.
- (44) Cacelli, I.; Cimoli, A.; Livotto, P. R.; Prampolini, G. An Automated Approach for the Parameterization of Accurate Inter-

molecular Force-Fields: Pyridine as a Case Study. *J. Comput. Chem.* **2012**, *33*, 1055–1067.

(45) Riley, K. E.; Pitoňák, M.; Černý, J.; Hobza, P. On the Structure and Geometry of Biomolecular Binding Motifs (Hydrogen-Bonding, Stacking, X–H···π): Wft and Dft Calculations. *J. Chem. Theory Comput.* **2010**, *6*, 66–80.

(46) Sherrill, C. D.; Takatani, T.; Hohenstein, E. An Assessment of Theoretical Methods for Nonbonded Interactions: Comparison to Complete Basis Set Limit Coupled-Cluster Potential Energy Curves for the Benzene Dimer, the Methane Dimer, Benzene–Methane, and Benzene–H<sub>2</sub>s. *J. Phys. Chem. A* **2009**, *113*, 10146–10159.

(47) Rutledge, L. R.; Durst, H. F.; Wetmore, S. D. Evidence for Stabilization of DNA/Rna–Protein Complexes Arising from Nucleobase–Amino Acid Stacking and T-Shaped Interactions. *J. Chem. Theory Comput.* **2009**, *5*, 1400–1410.

(48) Cacelli, I.; Lami, C. F.; Prampolini, G. Force-Field Modeling through Quantum Mechanical Calculations: Molecular Dynamics Simulations of a Nematicogenic Molecule in Its Condensed Phases. *J. Comput. Chem.* **2009**, *30*, 366–378.

(49) Riley, K.; Hobza, P. Assessment of the Mp2Method, Along with Several Basis Sets, for the Computation of Interaction Energies of Biologically Relevant Hydrogen Bonded and Dispersion Bound Complexes. *J. Phys. Chem. A* **2007**, *111*, 8257–8263.

(50) Cacelli, I.; Cinacchi, G.; Prampolini, G.; Tani, A. Computer Simulation of Solid and Liquid Benzene with an Atomistic Interaction Potential Derived from Ab Initio Calculations. *J. Am. Chem. Soc.* **2004**, *126*, 14278–14286.

(51) Tsuzuki, S.; Honda, K.; Uchimaru, T.; Mikami, M.; Tanabe, K. Origin of Attraction and Directionality of the π/π Interaction: Model Chemistry Calculations of Benzene Dimer Interaction. *J. Am. Chem. Soc.* **2002**, *124*, 104–112.

(52) Hobza, P.; Selzle, H. L.; Schlag, E. W. Potential Energy Surface for the Benzene Dimer. Results of Ab Initio Ccsd(T) Calculations Show Two Nearly Isoenergetic Structures: T-Shaped and Parallel-Displaced. *J. Phys. Chem.* **1996**, *100*, 18790–18794.

(53) Demovicova, L.; Hobza, P.; Rezac, J. Evaluation of Composite Schemes for Ccsdt(Q) Calculations of Interaction Energies of Noncovalent Complexes. *Phys. Chem. Chem. Phys.* **2014**, *16*, 19115–19121.

(54) Villani, G. Theoretical Investigation of the Hydrogen Transfer Mechanism in the Adenine-Thymine Base Pair. *Chem. Phys.* **2005**, *316*, 1–8.

(55) Mark, P.; Nilsson, L. Structure and Dynamics of the Tip3p, Spc, and Spc/E Water Models at 298 K. *J. Phys. Chem. A* **2001**, *105*, 9954–9960.

(56) Jorgensen, W. L. C.; Madura, J. D.; Impey, R. W.; Klein, M. L. Comparison of Simple Potential Functions for Simulating Liquid Water. *J. Chem. Phys.* **1983**, *79*, 926–935.

(57) Barone, V.; Cacelli, I.; De Mitri, N.; Licari, D.; Monti, S.; Prampolini, G. Joyce and Ulysses: Integrated and User-Friendly Tools for the Parameterization of Intramolecular Force Fields from Quantum Mechanical Data. *Phys. Chem. Chem. Phys.* **2013**, *15*, 3736–51.

(58) Cacelli, I.; Prampolini, G. Parametrization and Validation of Intramolecular Force Fields Derived from Dft Calculations. *J. Chem. Theory Comput.* **2007**, *3*, 1803–1817.

(59) Jorgensen, W. L.; Maxwell, D. S.; Tirado-Rives, J. Development and Testing of the Opls All-Atom Force Field on Conformational Energetics and Properties of Organic Liquids. *J. Am. Chem. Soc.* **1996**, *118*, 11225–11236.

(60) van der Spoel, D.; Lindahl, E.; Hess, B.; van Buuren, A. R.; Apol, E.; Meulenhoff, P.; Tieleman, D.; Sijbers, A.; Feenstra, K.; van Drunen, R.; Berendsen, H. GROMACS 4.5; Department of Biophysical Chemistry, University of Groningen: The Netherlands, 2010.

(61) Jorgensen, W. L.; Nguyen, T. B. Monte Carlo Simulations of the Hydration of Substituted Benzenes with Opls Potential Functions. *J. Comput. Chem.* **1993**, *14*, 195–205.